remote sensing

MDPI

Article

Study and Analysis of the Thunder Source Location Error Based on Acoustic Ray-Tracing

Jinyuan Guo [1], Caixia Wang [1,*], Jia Xu [1], Song Jia [1], Hui Yang [2], Zhuling Sun [3] and Xiaobao Wang [1]

[1] School of Applied Science, Beijing Information Science and Technology University, Beijing 102206, China; 2021021030@bistu.edu.cn (J.G.); 2023021105@bistu.edu.cn (J.X.); 2022021081@bistu.edu.cn (S.J.); bao@bistu.edu.cn (X.W.)
[2] Guangdong Provincial Key Laboratory of Geophysical High-Resolution Imaging Technology, Southern University of Science and Technology, Shenzhen 518055, China; yangh@sustech.edu.cn
[3] Institute of Atmospheric Physics, Chinese Academy of Sciences, Beijing 100029, China; sunzhuling@mail.iap.ac.cn
* Correspondence: caxwangee@bistu.edu.cn

Abstract: Error analysis and estimation of thunder source location results is a prerequisite for obtaining accurate location results of thunder sources, which is of great significance for a deeper understanding of the physical process of lightning channel discharges. Most of the thunder source location algorithms are based on the simplified model of the straight-line propagation of acoustic waves to determine the location of the thunder source; however, the acoustic wave is affected by the inhomogeneity of the atmosphere medium in the propagation process and its acoustic ray will be bent. Temperature and humidity are the main factors affecting the vertical distribution of the velocity of sound in the atmosphere, therefore, it is necessary to study the changes in location errors under the models of uniform vertical distribution of temperature only and uniform vertical distribution of humidity only. This paper focuses on the theory of acoustic ray-tracing in neglecting the presence of the wind and the acoustic attenuation and the theoretical derivation of the location error of thunder source inversion for the three models is carried out by using MATLAB R2019b programming. Then, simulation analysis and comparative study on the variation law of thunder source location error with the height of the source, ground temperature, ground humidity, and array position under the three models are carried out. The results of the study show that the maximum location error can be obtained from the straight-line propagation model, the location error obtained from the model of uniform vertical distribution of temperature only is the second, and the location error obtained from the model of uniform vertical distribution of humidity only is the least and can be negligible compared to the first two models. In the trend of error variation, the variation of location error with temperature and humidity is relatively flat in the first two models; however, the variation of location error with the height of the thunder source is more drastic, which can be more than 80%. The location error obtained from the array inversion closer to the thunder source increases linearly with the height of the thunder source, the location error obtained from the more distant array inversion shows a fast-decreasing trend at the height of the thunder source from 500 to 3500 m, and a flat trend above 3500 m. The location error varies relatively smoothly with the height of the thunder source, the ground temperature, and the ground humidity in the model of uniform vertical distribution of humidity only. In addition, the position of the array also has an important effect on lightning location. The further the horizontal distance from the source, the greater the location error will be obtained in the first two models, and when the thunder source is at a low height and detected at a long distance, the location error will be very large, so relevant data should be modified in actual observation.

Keywords: ray-tracing theory; thunder source location; location error; temperature distribution; humidity distribution

check for updates

Citation: Guo, J.; Wang, C.; Xu, J.; Jia, S.; Yang, H.; Sun, Z.; Wang, X. Study and Analysis of the Thunder Source Location Error Based on Acoustic Ray-Tracing. *Remote Sens.* **2024**, *16*, 4000. https://doi.org/10.3390/rs16214000

Academic Editors: Yuriy Kuleshov and Mike Wolff

Received: 28 June 2024
Revised: 29 September 2024
Accepted: 21 October 2024
Published: 28 October 2024

Copyright: © 2024 by the authors. Licensee MDPI, Basel, Switzerland. This article is an open access article distributed under the terms and conditions of the Creative Commons Attribution (CC BY) license (https://creativecommons.org/licenses/by/4.0/).

1. Introduction

Lightning is a violent discharge phenomenon that occurs in the atmosphere [1,2]. Lightning channel discharge is often accompanied by acoustic waves, light, electromagnetic waves, and other radiation [3], which has a destructive effect, triggering natural fires [4,5]. Utilizing acoustic, optical, electromagnetic, and other observations to locate the thunder source acts as an important means to study the occurrence, development, and discharge process of lightning channel [6], and accurate location is the premise and basis for studying the lightning channel and obtaining better results. Thus, it is important to study the location error for an in-depth understanding of the physical process of lightning discharge and for the prevention of the hazards of lightning [7–10].

During lightning, the air in the lightning channel will complete the process of intense heating to 15k °C–20k °C followed by rapid cooling, thus generating shock waves and evolving into the thunder heard by humans [11–13]. The study of the discharge process in lightning channels based on the location of thunder should be able to obtain information on the source of radiation that is different from that obtained from other observations, such as optical and electromagnetic location. If the baseline length of the observation array in the detection station is much shorter than the distance from the thunder source to the array, the thunder signal can be regarded as a plane wave transmitting to each array element. The direction information of the incident acoustic wave can be determined through the time difference of the arrival of the thunder signal to each array element, and the position of the thunder source can be inverted if there are more than one detection station, so as to realize the inversion of the lightning channels and further research [14–16]. In the 1970s, Few firstly utilized a Y-shaped station network consisting of four thunder detection stations to determine the three-dimensional location of the thunder source through the arrival time difference method [17]. Nakano reduced the baseline length of the station network to less than 10 m on the basis of this method, which reduced the interference of the environmental factors in the transmission of the thunder among the different stations [18]. And then, Bohannon optimized the location system, leading to more accurate results [19]. Arechiga et al. used an artificial-triggering lightning test to collect thunder signals and locate the thunder source through a microphone array system, and then compared it with the lightning mapping array (LMA) system [20]. Arechiga then developed a station network that contains a four-element microphone array station network with thunderstorm observations, in which the slow search and ranging method were applied to determine the 3-D region of lightning [21]. Zhang Han designed a single-station lightning location system, and the obtained results could better depict the lightning channel [22]. Qie et al. combined a 2-D VHF broadband interferometer with a 3-D acoustic imaging system to realize the inversion of the lightning channel [23]. Most of the above location studies assumed that the medium of the atmosphere was homogeneous, so that an acoustic wave was transmitted along a straight line in the air. Therefore, the model used was relatively simplified.

The real thunder signal transmitting in the air is affected by various environmental factors. The atmosphere produces absorption attenuation of the acoustic signal [24–27], and by the impact of temperature, humidity, and wind, the acoustic wave does not always transmit along a straight line [28–32], shown as Figure 1, so there may be significant errors between the lightning source location results of the straight-line propagation model and the real lightning source location. For this reason, the acoustic ray-tracing theory can be used to modify the error of the atmospheric environment on the location of the thunder by the horizontal stratification of the atmosphere. Few and Teer [28] and MacGorman [29,30] analyzed the problem of the refraction effect of the atmosphere on acoustic waves by stratifying the atmosphere horizontally in the simulation program and adding the parameter information of temperature gradient, wind speed, and wind shear, showing that the temperature gradient, wind speed, wind shear, and other factors would have a large impact on the thunder source location error. Few and Teer [28] reconstructed the structure of the lightning channel for specific observations and compared it with the optical observations, and confirmed that the refraction modification could better improve

the accuracy of location; MacGorman [29,30] found that the results obtained from the inversion differed from the development process of the real lightning channel through an observation experiment of summer thunderstorms, and it was hypothesized that the wind was one of the reasons for the error because of the wind shear on the ground during the observation. There is relatively little literature on the systematic research and modification of lightning source location errors in straight-line propagation models. With the deepening of research, this aspect of work urgently needs to be strengthened.

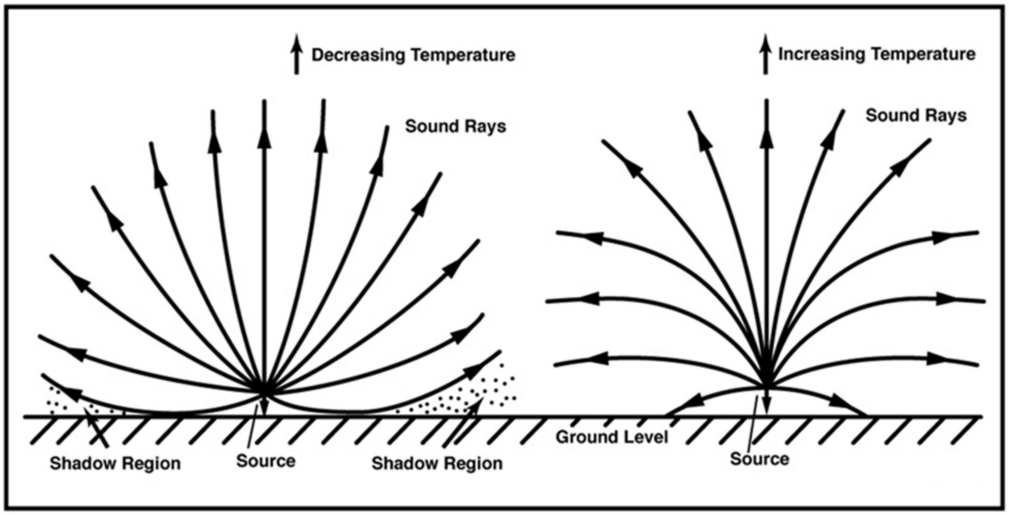


Figure 1. Direction of acoustic ray propagation corresponding to the model of temperature variation with height in windless atmosphere [32].

Considering the complex impact of wind, such as its intensity, direction, and distribution model, which can have a significant impact on the location results, we believe that studying wind separately in future work may be more suitable. In addition, the attenuation of acoustic waves during propagation can affect the amplitude of acoustic waves, and the amplitude attenuation will not affect the propagation path of acoustic waves and the location results of acoustic sources until it reaches zero. Therefore, the focus of this article is to study the influence of temperature and humidity distribution on location results, without considering wind and attenuation. Firstly, based on acoustic ray tracing, the principle of calculating the error caused by the vertical distribution of temperature and humidity on the location of lightning sources is theoretically derived in the article. Then, through MATLAB R2019b simulation and comparative analysis, the relative location error (RLE) of the thunder source location under different vertical distributions of temperature and humidity with the changes in the relationship of the height of the thunder source (HTS), the receiving array position (also expressed as the horizontal distance between the array and thunder source, denoted as X_n), the ground temperature (GT) and the ground relative humidity (GRH) is studied, which provides an important reference to the modification of the straight-line propagation model and is of great significance for the improvement of thunder source location accuracy.

2. Materials and Methods

Based on the models of vertical distribution of acoustic velocity in the atmosphere and Snell's law of refraction, this chapter introduces the calculation method of the acoustic wave transmission distance and the grazing angle that arrives at the receiving array obtained by stratifying the atmosphere horizontally. Then, this angle is used as the initial value of the inversion process to obtain the location result. Then, the RLE can be obtained. This part provides the theoretical support for the simulation of the succeeding chapters.

2.1. Vertical Distribution of Acoustic Velocity in the Atmosphere

In dry air, the relationship between the atmospheric acoustic velocity C and temperature T can be expressed as follows:

$$C = \sqrt{\frac{\gamma P}{\rho}} = \sqrt{\frac{\gamma R}{\mu} T} \tag{1}$$

In the equation, γ is the specific heat capacity ratio, P is the atmosphere pressure, μ is the molar mass of the gas, and R is the gas constant, but in fact the atmosphere contains water vapor, especially in thunderstorms, so the effect of humidity needs to be considered. According to the literature [33], the adiabatic acoustic velocity for humid air can be expressed as:

$$C = 331.5 \times \sqrt{\left(1 + \frac{t}{T_0}\right) \times \left(1 + 0.31 \times \frac{rP_s}{P}\right)} \tag{2}$$

In the equation, 331.5 is the acoustic velocity at 0 °C under a standard atmospheric pressure in dry air, the unit of which is m/s; T_0 denotes the absolute temperature at 0 °C, which is 273.15 K; r denotes the relative humidity of the atmosphere; P_s denotes the saturated vapor pressure at t °C, and P denotes the standard atmospheric pressure. According to the literature [31,34], the saturated vapor pressure can be expressed as:

$$P_s = 6.112 \times \exp\left(\frac{17.67 \times t}{t + 243.5}\right) \tag{3}$$

in which, the unit of P_s is millibars.

According to the literature [35], the relationship of atmospheric relative humidity with altitude can be expressed as:

$$r = \begin{cases} r_0 \times (1 - 0.2523 \times 0.001 \times h) & 0 \le h \le 2 \text{ km} \\ 0.4954 \times r_0 \times \exp\left(\frac{2 - 0.001 \times h}{1.861}\right) & 2 \text{ km} \le h < 8 \text{ km} \\ 0.0197 \times r_0 \times \exp\left(\frac{8 - 0.001 \times h}{1.158}\right) & h \ge 8 \text{ km} \end{cases} \tag{4}$$

in which, r_0 denotes relative humidity of the ground and h is the height.

In general, the atmospheric temperature decreases by 6 °C with every 1000 m of elevation [30]:

$$t = t_0 - \frac{h}{1000} \times 6 \tag{5}$$

From the above equations, the acoustic velocity in Earth's atmosphere varies at different altitudes, and when there is no wind, it is macroscopically characterized by horizontal stratification, i.e., the main parameters (temperature, humidity, and pressure) change with the altitude, and the horizontal direction is relatively homogeneous. As a result, the transmission of acoustic waves in the atmosphere is mainly affected by vertical distribution of the atmosphere. In the subsequent simulation and discussion, the acoustic velocity equation is mainly based on Equations (1)–(5), which study the vertical distribution of the acoustic velocity in the humid atmosphere and its influence on the location results.

2.2. Theory of Acoustic Ray Transmission

Based on the vertical distribution of the atmosphere, if the vertical height of the atmosphere is divided into a number of layers, each of which is thin enough, the acoustic ray from the thunder source will be refracted after passing through each layer, resulting in a bend of the acoustic ray.

2.2.1. The Eikonal Equation

The Eikonal equation can be used to describe the changes in the wavefront plane and normal in space during acoustic wave transmission, as well as the distribution of acoustic ray in space.

Assuming that the atmosphere is a stationary medium, the fluctuation equation for acoustic waves can be expressed as:

$$\frac{\partial^2 P}{\partial t^2} = C^2 \times \nabla^2 P \tag{6}$$

Its solution be expressed as:

$$P(x, y, z, t) = P_A(x, y, z) \times e^{j[k\varphi(x,y,z) - \omega t]} \tag{7}$$

In the equation, P_A denotes the acoustic pressure amplitude as a function of spatial position; $\varphi(x, y, z)$ denotes the phase; k is the wave number. If the amplitude does not vary rapidly in space, it can be further expressed as:

$$|\nabla \varphi| = \frac{\omega}{k_0 C} = \frac{C_0}{C} = n \tag{8}$$

In the equation, C_0 denotes the acoustic velocity at the reference point and n denotes the refractive index. Equation (8) is written as Eikonal equation [36,37] in the stationary atmosphere, which indicates that during the transmission of acoustic waves in space, the gradient $|\nabla \varphi|$ of the wavefront and the refractive index at each point are comparable.

2.2.2. Snell's Law of Refraction for Acoustic Ray Transmission

Acoustic ray follows Snell's law of refraction [38–40] and can be expressed as:

$$\frac{cos\alpha}{C} = \frac{cos\alpha_0}{C_0} = const \tag{9}$$

In the equation, α is the angle between the acoustic ray at any height and the horizontal Ox axis, defined as the grazing angle; α_0 and C_0 are, respectively, expressed as the initial grazing angle of the position of the thunder source and the acoustic velocity, as shown in Figure 2. According to Equations (1)–(5), if the vertical distribution of the acoustic velocity in the atmosphere is known, it can determine the grazing angle at any height, that is, the transmission direction of the acoustic wave.

Equation (9) can be further changed to:

$$ncos\alpha = cos\alpha_0 = \mathrm{A} \tag{10}$$

in which, A is a constant.

Due to $dz/dx = tan\alpha$, the differential equation of the acoustic ray can be obtained as:

$$\frac{dz}{dx} = \sqrt{\left(\frac{n}{\mathrm{A}}\right)^2 - 1} \tag{11}$$

The horizontal transmission distance of the acoustic ray can be obtained by solving Equation (11) differentially:

$$X = \sum_{m=1}^{M} \frac{\Delta z}{\sqrt{\left(\frac{n_m}{\mathrm{A}}\right)^2 - 1}} = \sum_{m=1}^{M} \frac{\Delta z}{\sqrt{\left(\frac{C_0}{C_m \mathrm{A}}\right)^2 - 1}} \tag{12}$$

In the equation, Δz denotes the thickness of the layer; n_m denotes the refractive index corresponding to each layer, and M denotes the total number of layers. The total horizontal

transmission distance of the acoustic ray can be obtained by adding up the horizontal transmission distance of each layer.

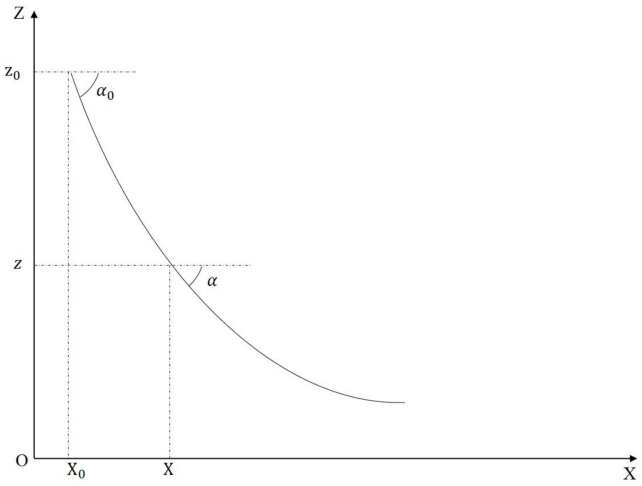


Figure 2. Schematic diagram of the acoustic ray trajectory. X_0 and Z_0 represent the horizontal and vertical position of the initial thunder source, respectively. α_0 represents the initial grazing angle. X and Z represent the horizontal and vertical position of the acoustic ray in propagation. α represents the propagation direction of the acoustic wave at any height.

2.3. Principle of RLE Calculation for Three Models

At any moment, the thunder source can be regarded as the point of the acoustic source. The vertical distribution of the atmospheric medium is assumed to follow a certain law, so according to Snell's law, the acoustic ray between the observation array at any position and the thunder source, initial grazing angle α_0 and the grazing angle of the acoustic ray reaching the array, can be determined uniquely.

According to Equations (1)–(5), the velocity of the acoustic wave varies with altitude, so after passing through each layer, the speed of the acoustic wave will change, and according to Equations (9) and (10), the direction of the acoustic ray will also change, which leads to the grazing angle received by the observation array not being equal to the initial angle of the thunder source, which is shown as the solid line in Figure 3.

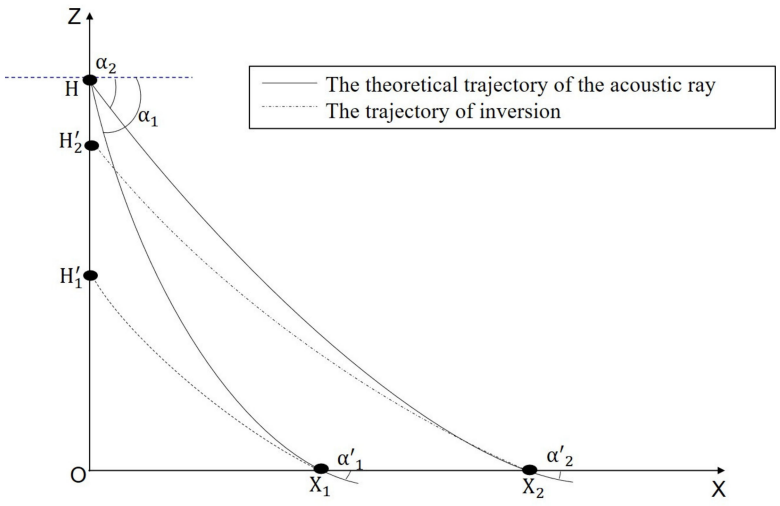


Figure 3. The theoretical trajectory of the acoustic ray and trajectory of inversion. X_n denotes the array position, H denotes the theoretical height of the thunder source, H'_n denotes the height of the inversion result for each array, α_n denotes the initial grazing angle corresponding to the array, α'_n denotes the receiving grazing angle.

In the process of inversing the thunder source location based on array observation data, the grazing angle received by the observation array can be used as the initial angle, and then by using Equations (9) and (10), the inversion height can be obtained when the cumulative horizontal propagation distance is X_n. If both the variation of atmospheric temperature and humidity with altitude in the inversion process complies with Equations (4) and (5), then the inversion height should be consistent with the theoretical height H of the thunder source, and the error is zero. Otherwise, the inversion trajectory will not conform to the theoretical acoustic ray, which is shown as the dotted line in Figure 3, so the inversion height H′ will not be consistent with the theoretical height H, denoted as $\Delta H = H - H'_n$, then the RLE, which equals $\frac{\Delta H}{H}$, can be obtained.

This paper aims to estimate the effect of vertical distribution of atmospheric temperature and humidity on RLE and its variation law, and then summarize the main influencing factors of location error, which can provide an important reference for error modification of simplified straight-line propagation model.

2.3.1. Calculation of the RLE in Straight-Line Propagation Model

Assuming that temperature and humidity are both equally distributed vertically, i.e., neither of them changes with altitude, and according to Equations (1)–(5), it can be concluded that the acoustic velocity is constant, then the acoustic ray can be regarded as a straight line without deflection. According to Figure 4, the inversion height can be obtained from the geometric relationship:

$$H'_n = X_n \times \tan \alpha'_n \tag{13}$$

In the equation, α'_n represents the grazing angle of the acoustic ray reaching the array.

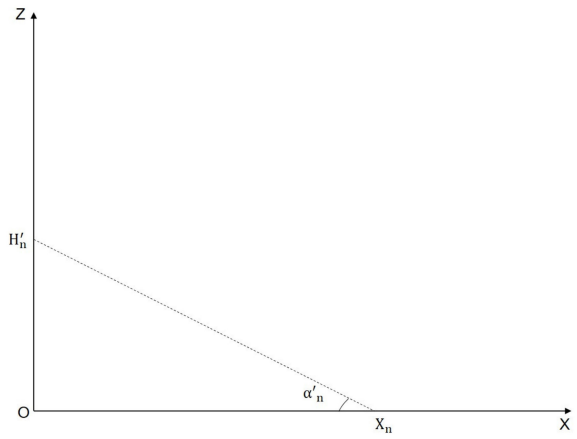


Figure 4. Schematic diagram of the RLE based on straight-line propagation model. α'_n denotes the receiving grazing angle, X_n denotes the position of the array, H'_n denotes inversion height.

2.3.2. Calculation of RLE in Uniform Vertical Distribution of Temperature Only

Assuming that the temperature at the ground is t_0 °C and only considering the stratification of humidity with altitude, i.e., the temperature is constant with altitude, then the expression for the acoustic velocity can be expressed as:

$$C = 331.5 \times \sqrt{\left(1 + \frac{t_0}{T_0}\right) \times \left(1 + 0.31 \times \frac{rP_s}{P}\right)} \tag{14}$$

Then, based on the atmospheric stratification, the horizontal transmission distance of each layer and the total distance of acoustic ray are obtained according to Equations (11) and (12) to obtain the height of the inversion.

2.3.3. Calculation of RLE in Uniform Vertical Distribution of Humidity Only

Assuming that the humidity at the ground is RH_0 and only considering the stratification of temperature with altitude, i.e., the humidity is constant with altitude, then the expression for the acoustic velocity can be expressed as:

$$C = 331.5 \times \sqrt{\left(1 + \frac{t}{T_0}\right) \times \left(1 + 0.31 \times \frac{RH_0 \times P_s}{P}\right)} \quad (15)$$

Then, based on the atmospheric stratification, the horizontal transmission distance of each layer and the total distance of the acoustic ray are obtained according to Equations (11) and (12) to obtain the height of the inversion.

3. Simulation Results and Analysis

This chapter focuses on the three models mentioned above by using MATLAB R2019b simulation. The thunder source occurring in the troposphere height range (0–10,000 m) is mainly studied. Then, the RLE obtained by using different atmospheric medium vertical distribution models in the inversion process of observation arrays with horizontal distances of 500 m, 2000 m, 3500 m, 5000 m, 6500 m, and 8000 m from the thunder source is estimated. At the same time, in order to better reflect the influence of the HTS, GT and GRH on RLE, horizontal and vertical comparisons were made on the RLE curves in each of the figures in Sections 3.1–3.3. The horizontal axis of these figures represents the HTS, GT, or GRH. The horizontal comparison is conducted by calculating the range of the RLE variation of the curve with respect to the x-axis, which uses the difference between the maximum and minimum values of the curve at a certain interval to represent it so as to obtain the degree of influence of the physical quantity of the horizontal axis on RLE. The vertical comparison is conducted and the RLE law varying with the array position is studied so as to obtain the RLE variation law with the array position. Then, the RLE variation law obtained from horizontal and vertical comparison is summarized and the main factors affecting the thunder source location are obtained.

3.1. Location Error of Straight-Line Propagation Model

3.1.1. The Variation Law of Location Error with the Height of Thunder Source

Assuming that GT is 30 °C and GRH is 0.8, HTS is taken from 500 m to 9500 m at 1000 m intervals. The RLE obtained from the inversion at position X_n is acquired and the simulation results obtained are shown in Figure 5.

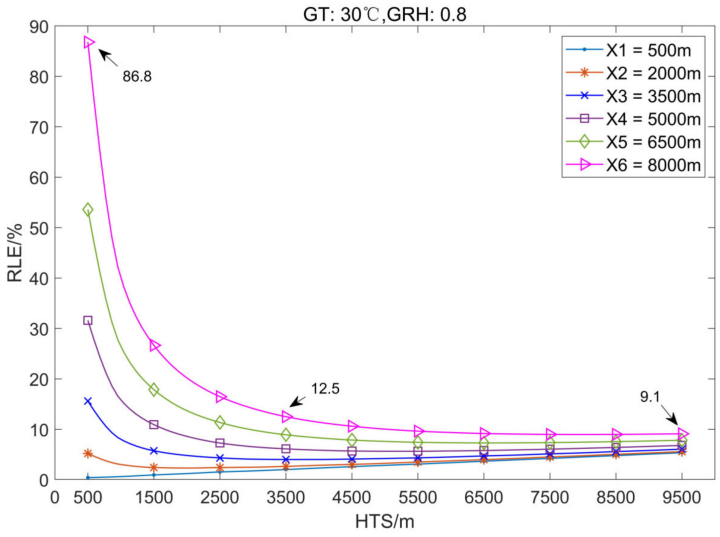


Figure 5. The variation of RLE with HTS in straight-line propagation model. Six curves represent the variation trend of the corresponding array position.

From Figure 5, when HTS is less than 3500 m, the RLE of the farther observation array decreases sharply with HTS, and the maximum RLE can change by about 70%, shown as the curve of the X_6 = 8000 m, which decreases from 86.8% to 12.5%; When HTS is over 3500 m, the RLE of each array changes gently with the increase of HTS, and the maximum RLE change is about 4%, shown as the curve of the X_6 = 8000 m, which decreases from 12.51% to 9.116%. It can be concluded that the RLE of the array with a farther horizontal distance from the thunder source is more affected by the variation of the HTS at a low altitude, while the RLE of the array with a closer horizontal distance from the thunder source is less affected by the thunder source at any height.

3.1.2. The Variation Law of Location Error with Ground Temperature

Assuming that HTS is 2500 m, GRH is 0.8, GT is taken from −20 °C to 50 °C at the interval of 10 °C. The RLE is acquired and the simulation results obtained are shown in Figure 6.

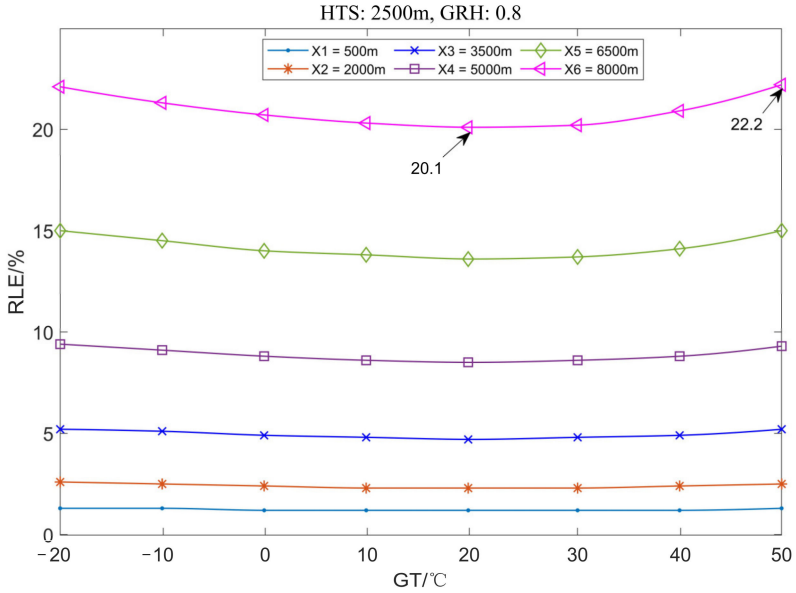


Figure 6. The variation of RLE with GT in straight-line propagation model. Six curves represent the variation trend of the corresponding array position.

From Figure 6, when the horizontal distance of the observing array is closer to the thunder source, the RLE is not obvious with the change of GT, which is almost unchanged. With the increase of the horizontal distance between the array and the thunder source, the RLE is increasingly obvious with the change of GT, for example, when the array position is 8000 m, it can be clearly seen that the RLE changes with GT and the maximum RLE variation is 2%, as shown as the curve of the X_6 = 8000 m, which varies from 20.1% to 22.2%. In addition, at the same GT, the RLE increases with the increase of the horizontal distance between the array and the thunder source, from about 1% to more than 20%.

3.1.3. The Variation Law of Location Error with Ground Humidity

Assuming that HTS is 2500 m, GT is 30 °C, and GRH is taken from 0.1 to 0.9 at the interval of 0.1. The RLE is acquired, and the simulation results are shown in Figure 7.

From Figure 7, the RLE does not change significantly with GRH, and the variation trend is relatively smooth, with a maximum RLE variation of 3%, as shown as the curve of the X_6 = 8000 m, which increases from 19.1% to 22.2%. At the same GRH, the RLE increases with the increase of the horizontal distance between the array and thunder source, from about 1% to more than 20%.

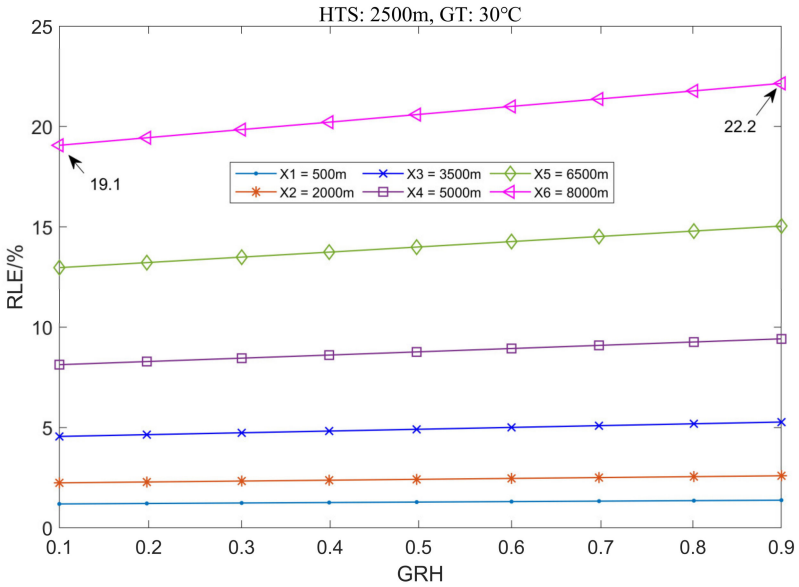


Figure 7. The variation of RLE with GRH in straight-line propagation model. Six curves represent the variation trend of the corresponding array position.

Combining the above three cases, in the model of the straight-line propagation, the RLE is greatly affected by the change of the HTS, followed by the change with GT, while the humidity has the least effect, which is almost unchanged with the humidity.

3.2. Location Error of the Model of Uniform Vertical Distribution of Temperature Only

3.2.1. The Variation Law of Location Error with the Height of the Thunder Source

Assuming that GT is 30 °C, GRH is 0.8, HTS is taken from 500 m to 9500 m at 1000 m intervals. The RLE is acquired and the simulation results obtained are shown in Figure 8.

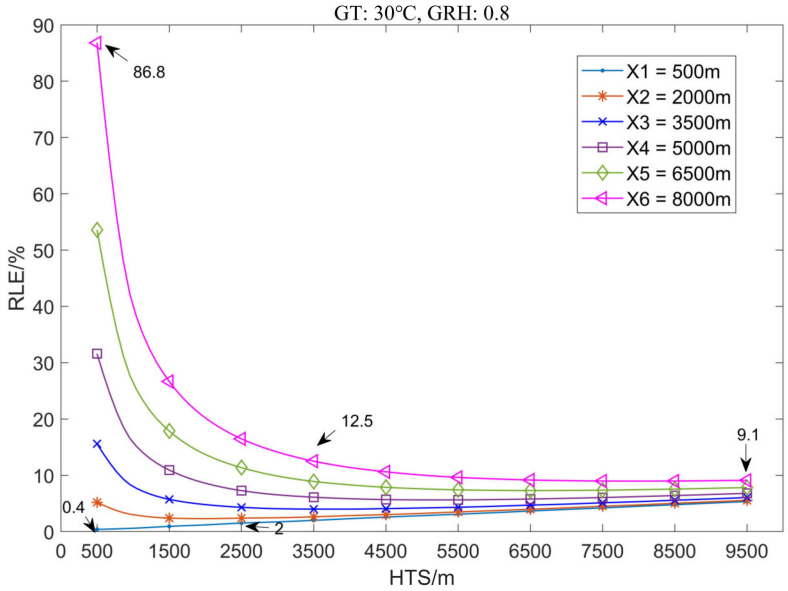


Figure 8. The variation of RLE with HTS in the model of uniform vertical distribution of temperature only. Six curves represent the variation trend of the corresponding array position.

From Figure 8, when HTS is above 3500 m, the RLE changes gently with the increase of HTS. The magnitude of the change is small, and the maximum RLE variation is about 4%, shown as the curve of the X_6 = 8000 m, which decreases from 12.5% to 9.1%; however, when HTS is between 500 m and 3500 m, the RLE of the farther observation array decreases

sharply with the increase of HTS, and the maximum RLE variation is about 70%, shown as the curve of the X_6 = 8000 m, which decreases from 86.8% to 12.5%. The RLE for the array with the closest horizontal distance from the thunder source changes gently with the increase of HTS and the magnitude of the change is small, with the minimum RLE variation being only 1.6%, as shown as the curve of the X_1 = 500 m, which increases from 0.4% to 2%.

3.2.2. The Variation Law of Location Error with Ground Temperature

Assuming that HTS is 2500 m, GRH is 0.8, GT is taken from −20 °C to 50 °C at the interval of 10 °C. The RLE is acquired and the simulation results obtained are shown in Figure 9.

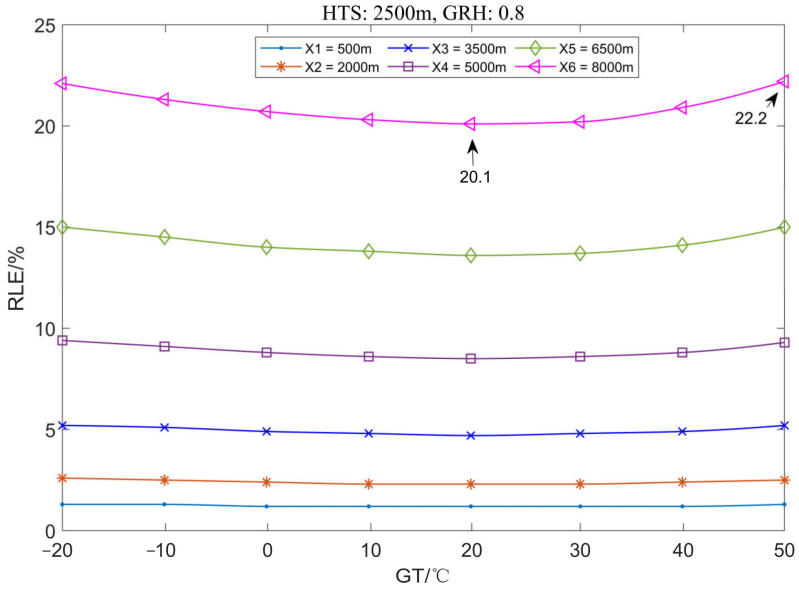


Figure 9. The variation of RLE with GT in the model of uniform vertical distribution of temperature only. Six curves represent the variation trend of the corresponding array position.

From Figure 9, the RLE does not change significantly with GT, and the variation trend is relatively smooth, with a maximum RLE variation of just 2%, shown as the curve of the X_6 = 8000 m, which varies from 20.1% to 22.2%. However, at the same GT, the RLE increases with the increase of the horizontal distance between the array and thunder source, from about 1% to more than 20%.

3.2.3. The Variation Law of Location Error with Ground Humidity

Assuming that HTS is 2500 m, GT is 30 °C, and GRH is taken from 0.1 to 0.9 at the interval of 0.1. The RLE is acquired and the simulation results obtained are shown in Figure 10.

From Figure 10, the RLE does not change significantly with GRH, and the variation trend is relatively smooth, with the maximum RLE variation being 1.5%, shown as the curve of the X_6 = 8000 m, which increases from 18.8% to 20.3%. However, in the same GRH, the RLE increases with the increase of the horizontal distance between the array and thunder source, from about 1% to more than 20%.

Combining the above three cases, in the model of uniform vertical distribution of temperature only, the RLE is most affected by the change of HTS, and less affected by the change in GT and GRH, with a smoother variation.

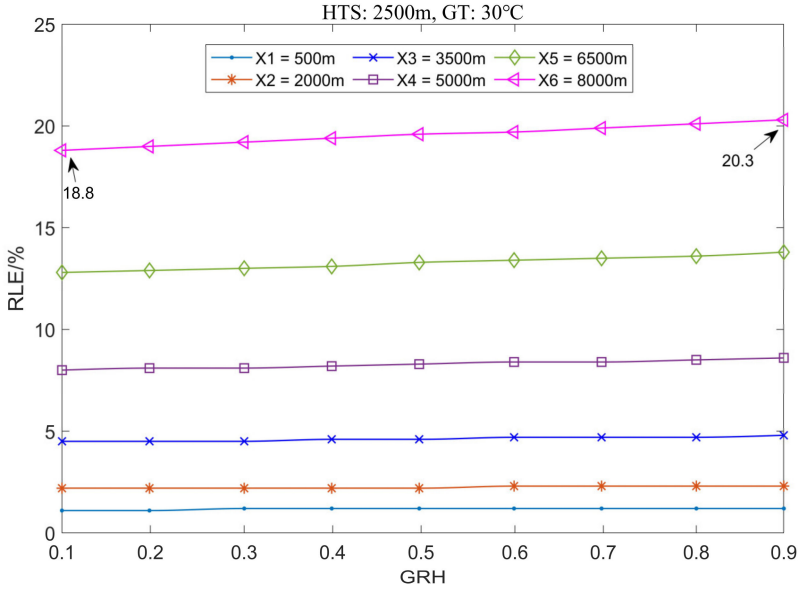


Figure 10. The variation of RLE with GRH in the model of uniform vertical distribution of temperature only. Six curves represent the variation trend of the corresponding array position.

3.3. Location Error of the Model of Uniform Vertical Distribution of Humidity Only

3.3.1. The Variation Law of Location Error with the Height of Thunder Source

Assuming that GT is 30 °C, GRH is 0.8, HTS is taken from 500 m to 9500 m at 1000 m intervals. The RLE is acquired and the simulation results obtained are shown in Figure 11.

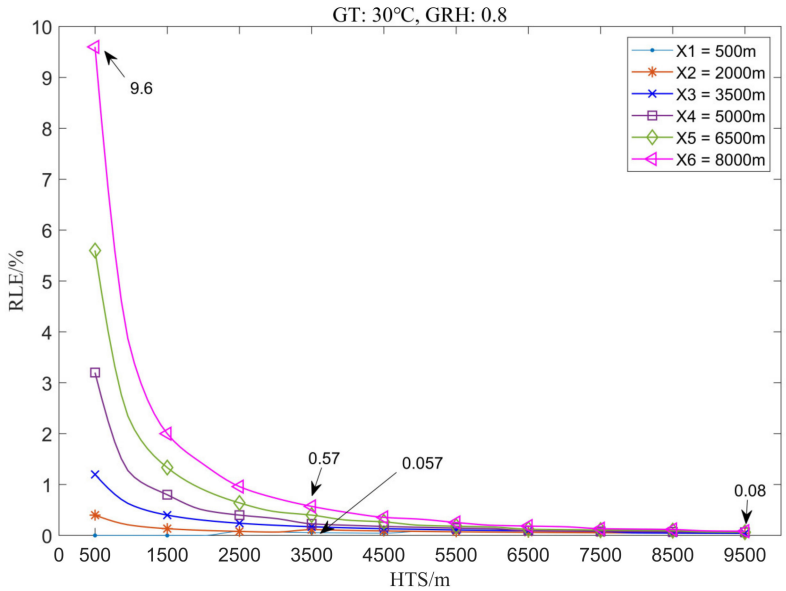


Figure 11. The variation of RLE with HTS in the model of uniform vertical distribution of humidity only. Six curves represent the variation trend of the corresponding array position.

From Figure 11, when HTS is above 3500 m, the RLE changes gently with the increase of HTS and the magnitude of the change is small, and the maximum RLE variation is about 0.5%, shown as the curve of the X_6 = 8000 m, which decreases from 0.57% to 0.08%. However, when HTS is between 500 m and 3500 m, the RLE of the farther observation array decreases sharply with the increase of HTS, and the maximum RLE variation is about 9%, shown as the curve of the X_6 = 8000 m, which decreases from 9.6% to 0.57%. The RLE of the array with the closest horizontal distance from the thunder source changes gently with the increase of HTS and the magnitude of the change is small, with the minimum RLE

variation being only 0.057%, shown as the curve of the X_1 = 500 m, which increases from 0% to 0.057%.

3.3.2. The Variation Law of Location Error with Ground Temperature

Assuming that HTS is 2500 m, GRH is 0.8, GT is taken from −20 °C to 50 °C at the interval of 10 °C. The RLE is acquired and the simulation results obtained are shown in Figure 12.

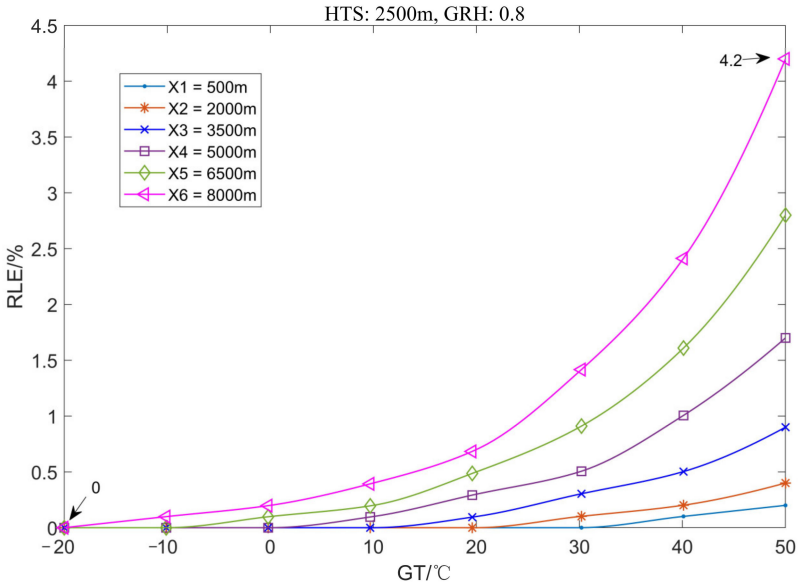


Figure 12. The variation of RLE with GT in the model of uniform vertical distribution of humidity only. Six curves represent the variation trend of the corresponding array position.

From Figure 12, the RLE does not change significantly with GT, and the variation trend is relatively smooth, with the maximum RLE variation of about 4%, shown as the curve of the X_6 = 8000 m, which increases from 0% to 4.2%. However, at the same GT, the RLE increases with the increase of the horizontal distance between the array and thunder source, from about 0.01% to about 4%.

3.3.3. The Variation Law of Location Error with Ground Humidity

Assuming that HTS is 2500 m, GT is 30 °C, and GRH is taken from 0.1 to 0.9 at the interval of 0.1. The RLE is acquired and the simulation results obtained are shown in Figure 13.

From Figure 13, with the increase of GRH, the RLE shows an upward trend, but the overall magnitude is weak, and the maximum RLE variation is 1%, shown as the curve of the X_6 = 8000 m, which increases from 0.1% to 1.1%. Moreover, the closer horizontal distance between the array and the thunder source, the RLE is more obvious in the form of step with the variation of GRH. In this simulation, only the vertical distribution of atmospheric humidity is considered uniform, but the atmospheric temperature changes with the altitude, indicating that the impact of humidity on acoustic velocity is much smaller than that of temperature, so the RLE changes slowly with the variation of GRH, showing a step-like change.

Combining the above three cases, in the model of uniform vertical distribution of humidity only, the RLE is most affected by the variation of HTS, and less affected by the variation of temperature and humidity, with a smoother variation.

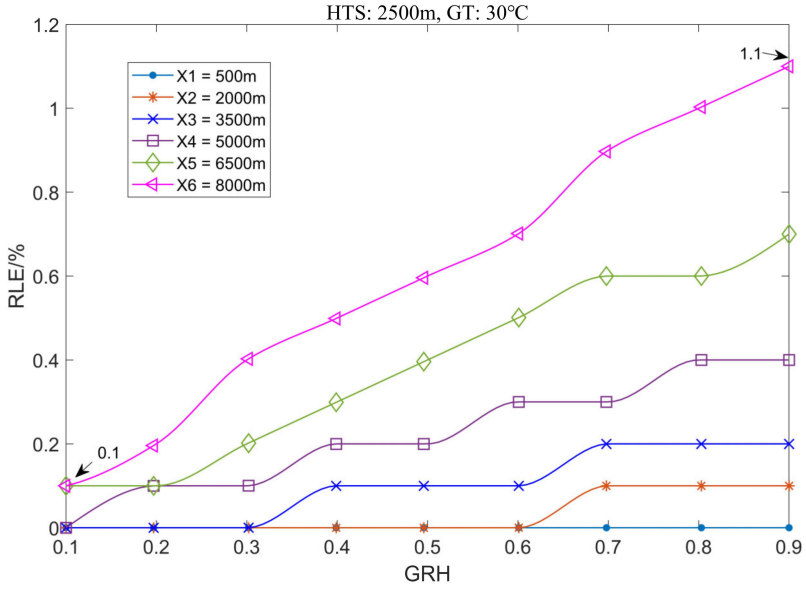


Figure 13. The variation of RLE with GRH in the model of uniform vertical distribution of humidity only. Six curves represent the variation trend of the corresponding array position.

3.4. Comparison of the Main Factors Affecting the Location Results

In order to further compare the variation law of the location error calculated by the above three models, the variation trend of RLE is plotted in a figure for comparison. In addition, due to the different location errors obtained from the inversion of the arrays at different positions, the following part is a comparative analysis of the inversion of the arrays at the position of 500 m, 3500 m, and 8000 m from the horizontal distance of the thunder source.

3.4.1. Effect of the Height of the Thunder Source on Location Error

When GT is 30 °C and GRH is 0.8, the curves of the RLE varies with HTS under three models are plotted in Figure 14. From Figure 14, when the array is close to the thunder source, the RLE obtained by the model of uniform vertical distribution of humidity only does not change significantly with HTS and tends to be zero, with a maximum RLE variation of only 0.08%, shown as Figure 14a. In contrast, the RLE obtained by straight-line propagation model and the model of uniform vertical distribution of temperature only increases linearly with HTS, with a maximum RLE variation of 5%, shown as Figure 14a.

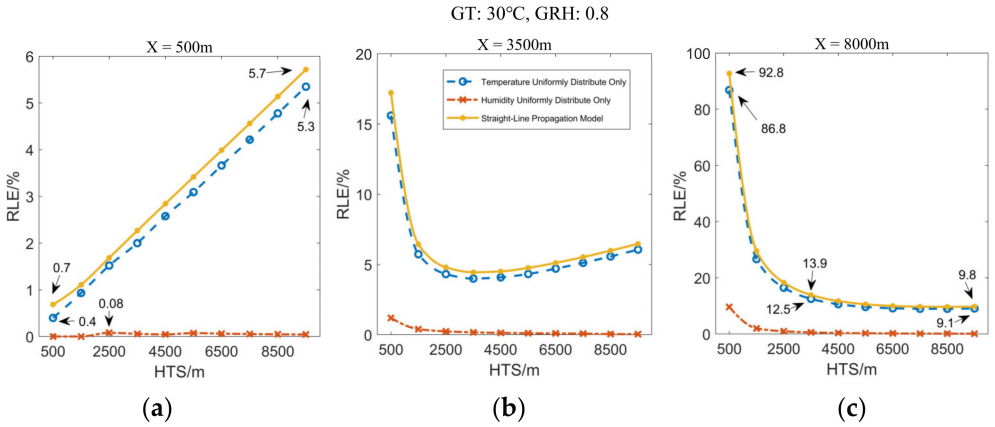


Figure 14. The variation of RLE of different vertical distribution models with HTS. (**a**) shows the variation of RLE at the array position of 500 m, (**b**) shows the variation of RLE at the array position of 3500 m, (**c**) shows the variation of RLE at the array position of 8000 m.

When the array is far away from the thunder source and HTS is below 3500 m, the RLE obtained by the model of uniform vertical distribution of humidity only, which affected by HTS, has a much bigger impact compared with that obtained from the inversion of the array in the near position. Meanwhile, the rate of the change of RLE obtained by the straight-line propagation model and the model of uniform vertical distribution of temperature only is more drastic with HTS and the maximum RLE variation can reach more than 70%, as shown as Figure 14c. When HTS is over 3500 m, the RLE obtained by the model of uniform vertical distribution of humidity only tends to be zero and the RLE obtained by the straight-line propagation model and the model of uniform vertical distribution of temperature only are gentler, for the maximum RLE variation is about 4%, also shown in Figure 14c.

In summary, it can be concluded that in the variation of the RLE with HTS, the RLE obtained by the model of uniform vertical distribution of humidity only is small and is less affected by the variation of HTS, whereas the RLE obtained by the straight-line propagation model and the model of uniform vertical distribution of temperature only are more affected by the variation of HTS.

3.4.2. Effect of the Ground Temperature on Location Error

When HTS is 2500 m and GRH is 0.8, the curves of the RLE varies with GT under three models, which are plotted in Figure 15. From Figure 15, it can be seen that in the variation of RLE with GT, the RLE obtained by the model of uniform vertical distribution of humidity only is small and changes gently with GT, with a maximum RLE variation of 4%, shown as Figure 15c; The RLE obtained by straight-line propagation model and the model of uniform vertical distribution of temperature only are relatively obvious, but also varies smoothly with GT, with maximum RLE variations of 6% and 2%, respectively, as shown as Figure 15c. In addition, a larger RLE will be obtained in the farther array especially in straight-line propagation model and the model of uniform vertical distribution of temperature only, which can reach more than 20% and is not negligible, shown as Figure 15c.

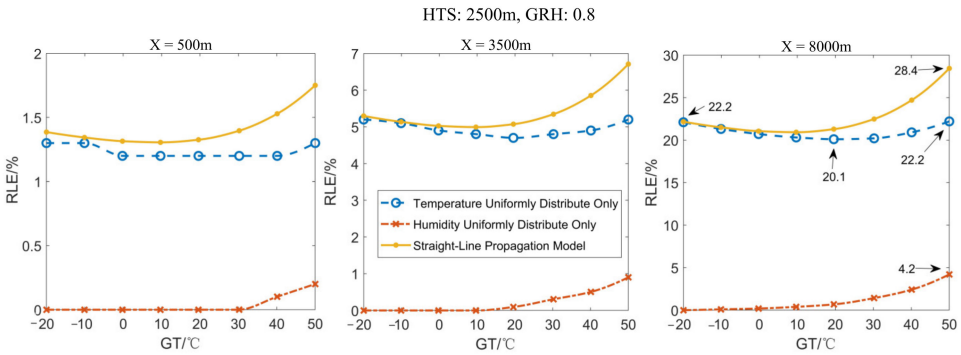


Figure 15. The variation of RLE of different vertical distribution models with GT. (**a**) shows the variation of RLE at the array position of 500 m, (**b**) shows the variation of RLE at the array position of 3500 m, (**c**) shows the variation of RLE at the array position of 8000 m.

3.4.3. Effect of the Ground Humidity on Location Error

When HTS is 2500 m and GT is 30 °C, the curves of the RLE varies with GRH under the three models, which are plotted in Figure 16. From Figure 16, it can be seen that in the variation of RLE with GRH, the RLE obtained by model of uniform vertical distribution of humidity only tends to be zero and changes gently with GRH, with a maximum RLE variation of about 1%, as shown as Figure 16c; The RLE obtained by straight-line propagation model and the model of uniform vertical distribution of temperature only are relatively obvious, but also varies smoothly with GRH, with maximum RLE variations of 1% and 3%, respectively, shown as Figure 16c. In addition, a larger RLE will be obtained in the farther array especially in straight-line propagation models and the model of uniform vertical

distribution of temperature only, which can reach more than 20% and is not negligible, as shown as Figure 16c.

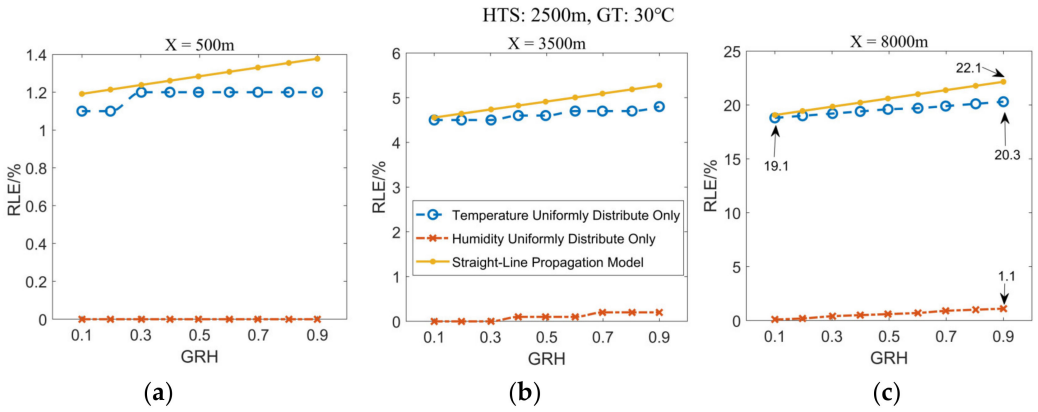


Figure 16. The variation of RLE of different vertical distribution models with GRH. (**a**) shows the variation of RLE at the array position of 500 m, (**b**) shows the variation of RLE at the array position of 3500 m, (**c**) shows the variation of RLE at the array position of 8000 m.

4. Discussion

From the perspective of acoustic ray-tracing, this paper theoretically deduces and simulates the RLE variation law of thunder source with the height of thunder source, ground temperature, and ground humidity obtained by three different vertical atmosphere models under no wind and no attenuation.

In previous research, Few, Teer, and MacGorman et al. [28–30] assumed that the location error caused by temperature gradient was small and almost negligible. However, the simulation results show that when the array position is far enough, the RLE obtained by the straight-line propagation model can reach more than 20%, especially when the thunder source is at a low height, the location error changes dramatically with the height of the thunder source, and the error is more obvious, even up to more than 80%, which cannot be ignored. Besides, previous studies mainly considered the influence of atmospheric medium on the time difference of the acoustic wave to each array, and thus obtained the influence of atmospheric medium on the location results, However, this paper mainly focuses on the propagation distance of the acoustic wave, by fixing the horizontal distance of acoustic wave propagation equals to the distance in inversion, which leads to the location result of inversion and the theoretical thunder source at the same horizontal position, so the location error can be compared more directly and comprehensively.

In the simulation process, we found that the influence of temperature on location error is much greater than that of humidity, for example by observing Figure 13, the variation curve of location error with humidity is obviously step-like shaped and the maximum value is only 1%, it can be inferred that under the model of uniform vertical distribution of atmospheric humidity, the acoustic velocity only changes with temperature, with little difference from the real acoustic velocity. However, humidity has little influence on the variation of acoustic velocity, so the location error does not change obviously with humidity, showing a step-like trend. In Figures 14–16, it can also be found that the location error curve obtained by the uniform vertical distribution of humidity only is much lower than the other two models and the error tends to be zero, which further demonstrates that the impact of humidity is less than temperature. In addition, the relative change between the initial grazing angle of the thunder source and the grazing angle arriving at the receiving array is calculated (GT is 30 °C and GRH is 0.8 for example), shown as Figure 17. It can be found that the overall variation of the curve is consistent with the above location error variation with the height of the thunder source. When HTS is between 500 m and 3500 m, the relative change of the grazing angle decreases rapidly with the increase of the height of the thunder source. If the parameters of the atmospheric medium are analyzed according

to the uniform vertical distribution model, the location result of inversion will change dramatically with the change of the height of the thunder source. With the increase of the height of the thunder source, the relative change of the grazing angle shows a gentle trend, which leads to the corresponding location error changing gently with the height of the thunder source. In addition, it can be found that the further the array position is, the greater the relative change of the grazing angle, which leads to the increase of the location error.

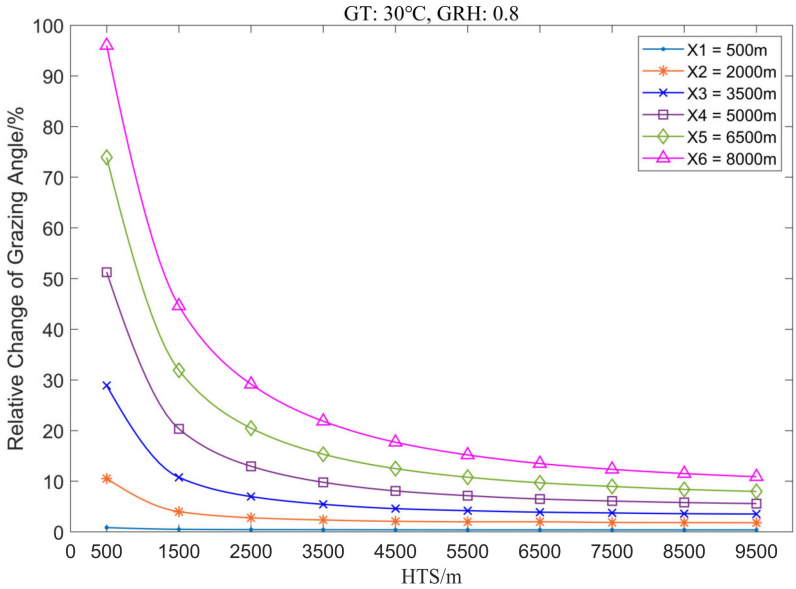


Figure 17. The variation of relative change of the grazing angle with HTS.

5. Conclusions

In order to research the effect of atmospheric temperature and humidity vertical distribution on thunder source location, this paper focuses on the theory of acoustic ray-tracing, explores the variation of the location error of inversion with the height of thunder source, ground temperature, ground humidity and the position of the array in the model of straight-line propagation, uniform vertical distribution of temperature only and uniform vertical distribution of humidity only. The main factors affecting the location of thunder source are obtained, which can provide an important reference on the modification of the simplified straight-line propagation model. The simulation results show that under the same conditions the location error obtained by the straight-line propagation model is the largest, the location error obtained by uniform vertical distribution of temperature only is the second, and the location error obtained by uniform vertical distribution of humidity only is the least, which tends to be zero. The magnitude of error obtained by the first two models is basically the same, which shows that the stratification of temperature has more obvious effects on thunder location than humidity stratification. Therefore, when modifying the error of the straight-line propagation model, it should be modified according to the stratification law of atmospheric temperature and humidity. In the trend of error variation, the error obtained by the straight-line propagation model and uniform vertical distribution of temperature only varies slightly with ground temperature and ground humidity, but it varies significantly with the height of the thunder source. The location error obtained by the model of uniform vertical distribution of humidity only varies gently with the height of the thunder source, ground temperature and ground humidity, and the error tends to be zero. In addition, the position of the array also has a significant impact on the thunder source location; when the array is far away from the thunder source and the height of the thunder source is low, the error obtained by straight-line propagation model and uniform vertical distribution of temperature only can be very large and the largest relative error can be about 90%.

Author Contributions: J.G.: writing, scheming, methodology, modeling and verifying; C.W.: review and editing; J.X.: editing; S.J.: editing; H.Y.: review and editing; Z.S.: review and editing, funding; X.W.: review and editing. All authors have read and agreed to the published version of the manuscript.

Funding: This work is supported by the R&D Program of Beijing Municipal Education Commission (Grant no. KZ20231123250), Guangdong Provincial Key Laboratory of Geophysical High-resolution Imaging Technology (Grant no. 2022B1212010002) and National Natural Science Foundation of China (Grant no. 41974122).

Data Availability Statement: The raw data supporting the conclusions of this article will be made available by the authors on request.

Conflicts of Interest: The authors declare no conflicts of interest.

References

1. Qie, X.S.; Qie, K.; Wei, L.; Zhu, K.X.; Sun, Z.L.; Yuan, S.F.; Jiang, R.B.; Zhang, H.B.; Xu, C. Significantly increased lightning activity over the Tibetan Plateau and its relation to thunderstorm genesis. *Geophys. Res. Lett.* **2022**, *49*, e2022GL099894. [CrossRef]
2. Sterpka, C.; Dwyer, J.; Liu, N.; Demers, N.; Demers, N.; Hare, B.M.; Scholten, O.; ter Veen, S. Ultra-Slow Discharges That Precede Lightning Initiation. *Geophys. Res. Lett.* **2022**, *49*, e2022GL101597. [CrossRef]
3. Wang, J.G.; Cao, J.X.; Cai, L.; Su, R.; Zhou, M.; Fan, Y.D.; Li, Q.X. Thunder acoustic signature for channel reconstruction in triggered lightning. *J. Appl. Phys.* **2022**, *132*, 123301. [CrossRef]
4. He, J.Y.; Loboda, T.V.; Chen, D.; French, N.H.F. Cloud-to-ground lightning and near-surface fire weather control wildfire occurrence in Arctic tundra. *Geophys. Res. Lett.* **2022**, *49*, e2021GL096814. [CrossRef]
5. Hessilt, T.D.; Abatzoglou, J.T.; Chen, Y.; Randerson, J.T.; Scholten, R.C.; van der Werf, G.; Veraverbeke, S. Future increases in lightning ignition efficiency and wildfire occurrence expected from drier fuels in boreal forest ecosystems of western North America. *Environ. Res. Lett.* **2022**, *17*, 054008. [CrossRef]
6. Wang, J.G.; Cao, J.X.; Cai, L.; Fan, Y.D.; Zhou, M.; Li, Q.X. Characteristics of Acoustic Response from Simulated Impulsive Lightning Current Discharge. *High. Voltage* **2019**, *4*, 221–227. [CrossRef]
7. Gallin, L.J.; Farges, T.; Marchiano, R.; Coulouvrat, F.; Defer, E.; Rison, W.; Schulz, W.; Nuret, M. Statistical analysis of storm electrical discharges reconstituted from a lightning mapping system, a lightning location system, and an acoustic array. *J. Geophys. Res. Atmos.* **2016**, *121*, 3929–3953. [CrossRef]
8. Hong, H.T.; Wang, B.S.; Lu, G.P.; Li, X.; Ge, Q.S.; Xie, A.; Wu, Y.; Qiu, X.X.; Chen, J. Tracking Lightning Through 3D Thunder Source Location with Distributed Acoustic Sensing. *J. Geophys. Res. Atmos.* **2024**, *129*, e2023JD038882. [CrossRef]
9. Zhang, Q.; Qie, X.; Wang, Z.; Zhang, T.; Zhao, Y.; Yang, J.; Kong, X. Characteristics and simulation of lightning current waveforms during one artificially triggered lightning. *Atmos. Res.* **2009**, *91*, 387–392. [CrossRef]
10. Qie, X.S.; Wu, X.K.; Yuan, T.; Bian, J.C.; Lu, D.R. Comprehensive pattern of deep convective systems over the Tibetan Plateau-south Asian monsoon region based on TRMM data. *J. Clim.* **2014**, *27*, 6612–6626. [CrossRef]
11. Rakov, V.A.; Uman, M.A. *Lightning: Physics and Effects*, 1st ed.; Cambridge University Press: Cambridge, UK, 2003; pp. 374–389.
12. Bodhika, J.A.P.; Dharmarathna, W.G.D.; Fernando, M.; Cooray, V. A preliminary study on characteristics of thunder pulses of lightning. In Proceedings of the International Conference on Lightning Protection, Shanghai, China, 11–18 October 2014.
13. Bodhika, J.A.P.; Dharmarathna, W.G.D.; Fernando, M.; Cooray, V. Localization of thunder source and reconstruction of lightning channel geometry using sound data. In Proceedings of the Asia-Pacific International Conference on Lightning, Chengdu, China, 1–4 November 2011.
14. Zhang, H.; Gu, S.Q.; Chen, J.H.; Zhao, C.; Wu, M.; Yan, B.W.; Wang, Y. Single-Station-Based Lightning Mapping System with Electromagnetic and Thunder Signals. *IEEE Trans. Compon. Packag. Manuf. Technol.* **2019**, *47*, 1421–1428. [CrossRef]
15. Bestard, D.; Coulouvrat, F.; Farges, T.; Mlynarczyk, J. Acoustical power of lightning flashes. *J. Geophys. Res. Atmos.* **2023**, *128*, e2023JD038714. [CrossRef]
16. Zhang, H. A Single-Station-Based 3D Lightning Channel Location Method by Using Differential Arrival Time of Thunder. Master's Thesis, Chinese Academy of Meteorological Sciences, Beijing, China, 2011.
17. Few, A.A. Lightning channel reconstruction from thunder measurement. *Geophys. Res.* **1970**, *75*, 7515–7523. [CrossRef]
18. Nakano, M. Characteristic of lightning channel in thunderclouds determined by thunder. *J. Meteorol. Soc. JPN* **1976**, *54*, 441–447. [CrossRef]
19. Bohannon, J.L. Infrasonic Pulses from Thunderstorms. Master's Thesis, Rise University, Houston, TX, USA, 1978.
20. Arechiga, R.O.; Johnson, J.B.; Edens, H.E.; Thomas, R.J.; Rison, W. Acoustic localization of triggered lightning. *J. Geophys. Res. Atmos.* **2011**, *116*, D09103-1–D09103-11. [CrossRef]
21. Johnson, J.B.; Arechiga, R.O.; Thomas, R.J.; Edens, H.E.; Anderson, J.; Johnson, R. Imaging thunder. *Geophys. Res. Lett.* **2011**, *38*, 1–7. [CrossRef]
22. Zhang, H.; Wang, D.H.; Lu, W.T.; Meng, Q.; Zhang, Y.J. A single station-based 3D lightning channel location system by using differential arrival time of thunder. *Plateau Meteorol.* **2012**, *31*, 209–217. [CrossRef]

23. Qiu, S.; Zhou, B.H.; Shi, L.H. Synchronized observations of cloud-to-ground lightning using VHF broadband interferometer and acoustic arrays. *J. Geophys. Res.* **2012**, *117*, 1–9. [CrossRef]
24. Harris, C.M. Absorption of Sound in Air versus Humidity and Temperature. *J. Acoust. Soc. Am.* **1966**, *40*, 148–159. [CrossRef]
25. Lacroix, A.; Coulouvrat, F.; Marchiano, R.; Farges, T.; Ripoll, J.F. Acoustical Energy of Return Strokes: A Comparison Between a Statistical Model and Measurements. *Geophys. Res. Lett.* **2019**, *46*, 11479–11489. [CrossRef]
26. Hong, T.K.; Park, S.; Chung, D.C.; Kim, B. Inversion of acoustic thunder source spectral model from thunder-induced seismic waves in megacity. *Geophys. J. Int.* **2023**, *233*, 107–126. [CrossRef]
27. Qiao, J.T. Research on Thunder Acoustic Signal Characteristics. Master's Thesis, Shaanxi Normal University, Xi'an, China, 2016.
28. Few, A.A.; Teer, T.L. The accuracy of acoustic reconstructions of lightning channels. *J. Geophys. Res.* **1974**, *79*, 5007–5011. [CrossRef]
29. MacGorman, D.R. Lightning Location in a Colorado Thunderstorm. Master's Thesis, Rice University, Houston, TX, USA, 1977.
30. MacGorman, D.R. Lightning Location in a Storm with Strong Wind Shear. Ph.D. Thesis, Rice University, Houston, TX, USA, 1978.
31. Sheng, P.X.; Mao, J.T.; Li, J.G.; Zhang, A.C.; Sang, J.G.; Pan, N.X. *Atmospheric Physics*, 1st ed.; Peking University Press: Beijing, China, 2003; pp. 486–495.
32. Simanek, D. Sound Reasons: The Answers. Available online: https://www.spsnational.org/the-sps-observer/winter/2015/sound-reasons-answers (accessed on 27 June 2024).
33. Wong, G.S.K.; Embleton, T.F.W. Variation of the speed of sound in air with humidity and temperature. *J. Acoust. Soc. Am.* **1985**, *77*, 1710–1712. [CrossRef]
34. Bolton, D. The computation of equivalent potential temperature. *Mon. Wea Rew* **1980**, *108*, 1046–1053. [CrossRef]
35. Guo, X.D.; Zuo, Z.G.; Yue, S.; Hong, P. Theoretical Model Analysis of the Effective Range of an Infrared Point Target Detection System. *Infrared* **2019**, *40*, 18–25.
36. Kornhauser, E.T. Ray theory for moving fluids. *J. Acoust. Soc. Am.* **1953**, *25*, 945–949. [CrossRef]
37. Thompson, R.J. Ray theory for an inhomogeneous moving medium. *J. Acoust. Soc. Am.* **1972**, *51*, 1675–1682. [CrossRef]
38. Shirley, J.W. An Early Experimental Determination of Snell's Law. *Am. J. Phys.* **1951**, *19*, 507. [CrossRef]
39. Son, K.T.; Lee, C.C. Design and Reliability of Acoustic Wedge Transducer Assemblies for Outdoor Touch Panels. *IEEE Trans. Compon. Packag. Manuf. Technol.* **2011**, *1*, 1178–1185. [CrossRef]
40. Hohenwarter, D.; Jelinek, F. Snell's Law of Refraction and Sound Rays for a Moving Medium. *Acta Acust. United Acust.* **1999**, *86*, 1. [CrossRef]

Disclaimer/Publisher's Note: The statements, opinions and data contained in all publications are solely those of the individual author(s) and contributor(s) and not of MDPI and/or the editor(s). MDPI and/or the editor(s) disclaim responsibility for any injury to people or property resulting from any ideas, methods, instructions or products referred to in the content.